8. P. Goldreich and J. Kwan, *ibid.* **189**, 441 (1974); N. Z. Scoville and P. M. Solomon, *Astrophys. J. Lett.* **187**, 67 (1975).
9. A. A. Penzias, *Science* **208**, 663 (1980).
10. J. H. Black and S. P. Willner, *Astrophys. J.* **279**, 673 (1984).
11. G. Neugebauer *et al.*, *Astrophys. J. Lett.* **278**, 1 (1984).
12. T. M. Dame and P. Thaddeus, *Astrophys. J.* **297**, 751 (1985).
13. E. E. Barnard, in *Photographic Atlas of Selected Regions of the Milky Way*, E. B. Frost and M. R. Calverd, Eds. (Carnegie Institution of Washington, Washington, DC, 1927); B. Bok and E. Reilly, *Astrophys. J.* **105**, 255 (1947).
14. R. L. Dickman and D. P. Clemens, *Astrophys. J.* **271**, 143 (1983); P. C. Meyers and P. J. Benson, *ibid.* **266**, 309 (1983); P. C. Meyers, *ibid.* **270**, 105 (1983); P. J. Benson, P. C. Meyers, E. L. Wright, *Astrophys. J. Lett.* **279**, 27 (1984).
15. L. Blitz, L. Magnani, L. Mundy, *Astrophys. J. Lett.* **282**, L9 (1984).
16. G. Baran, thesis, Columbia University (1981).
17. A. Moneti *et al.*, *Astrophys. J.* **282**, 508 (1984); F. J. Vrba, S. E. Strom, K. M. Strom, *Astron. J.* **81**, 958 (1976).
18. M. Cohen and L. Kuhi, *Astrophys. J. Suppl.* **41**, 743 (1979).
19. L. Blitz and A. A. Stark, *Astrophys. J.*, in press.
20. J. Bally and N. Z. Scoville, *ibid.* **239**, 121 (1980); C. J. Lada, B. G. Elmegreen, L. Blitz, in *Protostars and Planets*, T. Gehrels, Ed. (Univ. of Arizona Press, Tucson, 1984), pp. 341–367.
21. R. S. Cohen *et al.*, *Astrophys. J. Lett.* **290**, 15 (1985).
22. B. Zuckerman, *Annu. Rev. Astron. Astrophys.* **18**, 263 (1980); G. R. Knapp and M. Morris, *Astrophys. J.* **292**, 640 (1985).
23. R. D. Gehrz and N. J. Woolf, *Astrophys. J.* **165**, 285 (1971).
24. D. B. Sanders, P. M. Solomon, N. Z. Scoville, *ibid.* **276**, 182 (1985); T. M. Dame, thesis, Columbia University (1983).
25. D. B. Sanders, N. Z. Scoville, P. M. Solomon, *Astrophys. J.* **289**, 373 (1985); A. A. Stark, thesis, Princeton University (1979).
26. P. G. Goldsmith and W. D. Langer, *Astrophys. J.* **222**, 881 (1978).
27. G. M. Tielens and D. Hollenbach, *ibid.* **291**, 722 (1985).
28. L. F. Smith, P. Biermann, P. G. Mezger, *Astron. Astrophys.* **66**, 65 (1978); B. M. Tinsley, *Astrophys. J.* **208**, 797 (1976).
29. T. H. Troland and C. Heiles, *Astrophys. J. Lett.* **260**, 23 (1982); S. S. Hansen, *Astrophys. J.* **260**, 104 (1982); M. Dragovan, thesis, University of Chicago (1985).
30. A. A. Stark and L. Blitz, *Astrophys. J. Lett.* **225**, 15 (1978).
31. G. B. Field and W. C. Saslaw, *Astrophys. J.* **142**, 568 (1965).
32. J. Kwan, *ibid.* **229**, 567 (1979); N. Z. Scoville and K. Hersch, *ibid.*, p. 578.
33. L. Blitz and F. Shu, *ibid.* **238**, 148 (1980).
34. W. D. Langer, *ibid.* **225**, 860 (1978); in *Birth and Infancy of Stars*, R. Lucas, A. Omont, R. Stora, Eds. (North-Holland, Amsterdam, 1985), pp. 279–348.
35. J. Bally and C. J. Lada, *Astrophys. J.* **265**, 154 (1983); J. Welch *et al.*, *Science* **228**, 1389 (1985).
36. R. Mundt and J. W. Fried, *Astrophys. J. Lett.* **274**, 83 (1983).
37. M. J. Reid and J. M. Moran, *Annu. Rev. Astron. Astrophys.* **19**, 231 (1981).
38. C. Norman and J. Silk, *Astrophys. J.* **238**, 158 (1980).
39. L. Spitzer, *Physical Processes in the Interstellar Medium* (Wiley, New York, 1978).
40. B. G. Elmegreen and C. J. Lada, *Astrophys. J.* **214**, 725 (1977).
41. C. J. Lada, M. Margulis, D. Dearborn, *ibid.* **285**, 141 (1984).
42. C. J. Lada and B. A. Wilking, *ibid.* **287**, 610 (1984).
43. R. S. Cohen *et al.*, *Astrophys. J. Lett.* **239**, 53 (1980).
44. J. E. Gunn, in *Active Galactic Nuclei*, C. Hazard and S. Mitton, Eds. (Cambridge Univ. Press, Cambridge, 1979), p. 213; E. Bajaja *et al.*, *Astron. Astrophys.* **141**, 309 (1984).
45. J. Bally *et al.*, in preparation; G. Heiligman, thesis, Princeton University (1982); J. T. Armstrong and A. H. Barrett, *Astrophys. J. Suppl.* **57**, 535 (1984).
46. I. Gatley *et al.*, *Mon. Not. R. Astron. Soc.* **210**, 565 (1985); H. S. Liszt, W. B. Burton, J. M. van der Hulst, *Astron. Astrophys.* **142**, 237 (1985).
47. T. M. Bania, *Astrophys. J.* **216**, 381 (1977).
48. J. Oort, *Annu. Rev. Astron. Astrophys.* **15**, 295 (1977).
49. L. Spitzer and M. Schwarzschild, *Astrophys. J.* **114**, 385 (1951).
50. I. F. Mirabel and R. Morras, *ibid.* **279**, 86 (1984).
51. F. Verter, thesis, Princeton University (1983).
52. J. Young *et al.*, *Astrophys. J. Lett.* **287**, 65 (1984).
53. J. H. Bieging *et al.*, *Astrophys. J.* **247**, 443 (1981).
54. J. Young, N. Z. Scoville, E. Brady, *ibid.* **288**, 487 (1985); A. A. Stark *et al.*, in preparation.

Research Articles

Molecular Genetics of Human Color Vision: The Genes Encoding Blue, Green, and Red Pigments

JEREMY NATHANS, DARCY THOMAS, DAVID S. HOGNESS

Human color vision is based on three light-sensitive pigments. The isolation and sequencing of genomic and complementary DNA clones that encode the apoproteins of these three pigments are described. The deduced amino acid sequences show 41 ± 1 percent identity with rhodopsin. The red and green pigments show 96 percent mutual identity but only 43 percent identity with the blue pigment. Green pigment genes vary in number among color-normal individuals and, together with a single red pigment gene, are proposed to reside in a head-to-tail tandem array within the X chromosome.

VISUAL PIGMENTS ARE THE LIGHT-ABSORBING MOLECULES that mediate vision. They consist of an apoprotein, opsin, that is covalently linked to 11-*cis*-retinal or, in rare instances, 11-*cis*-dehydroretinal. Visual pigments are integral membrane proteins: in vertebrates they reside in the plasma and disk membranes of the photoreceptor outer segment. Vision begins when a photon is absorbed by a visual pigment, isomerizing retinal from the 11-*cis* to the all-*trans* configuration. Photoisomerized retinal triggers a series of conformational changes in the attached apoprotein which creates or unveils an enzymatic site on its cytosolic face. During its brief lifetime one enzymatically active visual pigment catalyzes the conversion of several hundred second messengers from an inert to an active state. This conversion is the first step in a cascade of enzymatic reactions that ultimately produces a neural signal (*1*).

All visual pigment absorption spectra have nearly the same characteristic bell shape (*2*). Each pigment is therefore specified by its wavelength of maximal absorption. The three pigments that mediate human color vision have absorption maxima at approxi-

The authors are in the Department of Biochemistry, Stanford University School of Medicine, Stanford, CA 94305. Reprint requests should be addressed to David S. Hogness.

mately 420 nm (the blue-sensitive pigment), 530 nm (the green-sensitive pigment), and 560 nm (the red-sensitive pigment) (*3*). These three pigments are referred to as cone pigments because they reside in those photoreceptor cells with cone-shaped outer segments. A fourth pigment, rhodopsin, that mediates vision in dim light and absorbs maximally at 495 nm, is found in those photoreceptors with rod-shaped outer segments.

Biochemical studies have usually been focused on rhodopsin, which in most mammals constitutes the most abundant visual pigment. Although, psychophysical and microspectrophotometric experiments have provided a wealth of data concerning the absorption properties of the cone pigments (*3*), we know little about their structures. However, it seems reasonable to suppose that the different visual pigments are structurally homologous and have arisen from a common ancestor.

In this article we describe a test of the hypothesis that human color vision is mediated by a family of rhodopsin-like molecules, the apoproteins of which are encoded by the corresponding members of a family of genes. In the accompanying article (*4*) we describe a test of a related hypothesis that the common inherited variations in human color vision (color blindness) are due to mutations in the members of this gene family. Our experimental approach is to isolate these genes by molecular cloning and determine their structures in both normal and mutant individuals. We reasoned that if the different visual pigments evolved from a common ancestor, then the genes that encode them may retain a degree of sequence homology to the ancestral gene and hence to each other. If this degree of homology is sufficiently high, then a molecular clone of one visual pigment gene could be used to isolate the others by hybridization at low stringency.

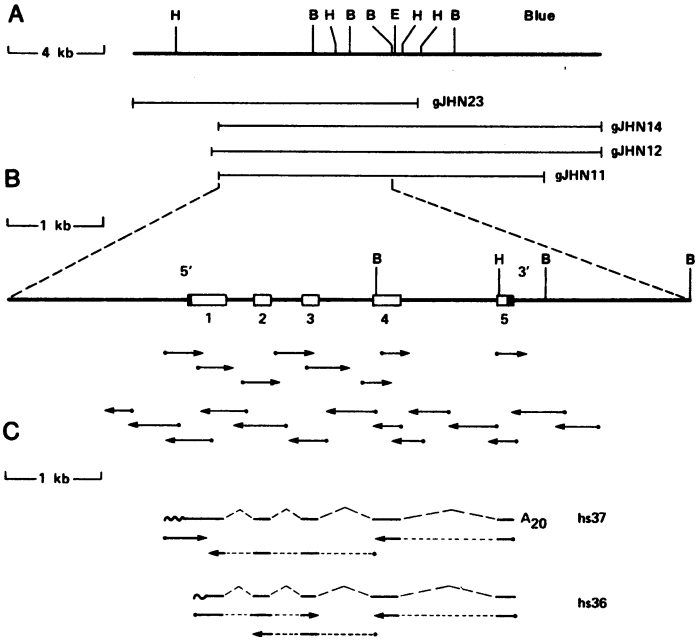

Fig. 1. Structure of the blue pigment gene. (A) The four cloned genomic segments (gJHN11, gJHN12, gJHN14, and gJHN23) are aligned beneath a map of the chromosomal DNA from which they derive. They were isolated from a human germline DNA library (from J.N.) prepared as described (*6*). The library was screened with a fragment of a bovine rhodopsin cDNA clone, bd20 [nt 56 to 1164; see figure 6 in (*5*)], which contains the entire coding region. Nitrocellulose plaque filters (*21*) were hybridized for 24 hours at 42°C with nick-translated (*22*) probe (10^6 count/min per milliliter) in 10 percent formamide, 10 percent dextran sulfate, 1.0*M* NaCl, 50 m*M* NaH_2PO_4, *p*H 7, 5 m*M* EDTA, and 1 percent sodium dodecyl sulfate, and then washed with several changes of the same buffer (without the probe and dextran sulfate) at 42°C for several hours. (B) Exons are represented by boxes and are numbered. Open boxes represent coding regions and closed boxes represent noncoding regions. Each arrow represents the extent of sequence determined (*23*) from a DNA strand of polarity 3′ to 5′ in the direction of the arrow, whose end was labeled at the site of the dot. The sequencing strategy involves the construction of a set of nested deletions as described in (*6*). (C) The structures of two cDNA clones (hs36 and hs37) are shown; these clones were isolated from a human retina cDNA library constructed in λgt10 (*24*) as described (*5*). These two recombinants were isolated by hybridization under standard conditions (*25*) to a probe derived from the first exon. Dashed lines represent intronic regions not present in the cDNA clones. The 3′ end of hs37 contains a stretch of 20 adenosines (A_{20}) not present in the genomic sequence; they presumably derive from copying of the poly(A) tract of the mRNA and therefore define the 3′ end of that gene. Both cDNA clones contain small regions of DNA at their 5′ ends (wavy lines) that do not correspond to genomic sequences and appear to be artifacts of the cDNA cloning method. B, Bam HI; E, Eco RI; H, Hind III.

Table 1. Percentage sequence homology and identity in pairwise comparisons of human visual pigments. The values below the 100 percent diagonal represent the percentage of amino acids that are identical, while those above this diagonal represent the percentage of amino acids that are identical or homologous. In this analysis and in that shown in Fig. 12, two amino acids are considered homologous and their substitution conservative, if they are found together in one of the following classes: (class 1) alanine, valine, leucine, isoleucine, proline, phenylalanine, tryptophan, methionine, glycine, cysteine; (class 2) serine, threonine, cysteine, tyrosine, asparagine, glutamine; (class 3) aspartic acid, glutamic acid; (class 4) lysine, arginine, histidine; (class 5) phenylalanine, tyrosine, tryptophan; (class 6) histidine, tryptophan. [see (*12*) and (*32*)].

	Percentage			
	Rhodopsin	Blue	Red	Green
Rhodopsin	100	75	73	73
Blue	42	100	79	79
Red	40	43	100	99
Green	41	44	96	100

As a first step we isolated and characterized complementary DNA (cDNA) and genomic DNA clones encoding bovine rhodopsin, the best-studied visual pigment (*5*). We then used the DNA sequence encoding bovine rhodopsin to probe libraries of human genomic DNA. [These genomic libraries and all of the cloned human genomic DNA described herein were derived from germline DNA of one of us (J.N.), a male who has normal color vision.] In our initial screen, conducted at approximately 40 degrees (Celsius) below the melting temperature of a perfect duplex, we isolated only clones derived from the gene encoding human rhodopsin (*6*). These data and the results of genomic DNA blots hybridized under similar conditions convinced us that the human rhodopsin gene is the only segment of human DNA that exhibits a strong sequence homology to the bovine rhodopsin coding region.

To increase the likelihood of detecting weakly cross-hybridizing sequences we screened 5×10^6 independent genomic clones at approximately 55 degrees below the melting temperature of a perfect duplex and in the presence of 10 percent dextran sulfate. The hybridizing clones from this screen fell into three classes defined by their restriction maps and hybridization intensities. The first class, with 21 members, was derived from the gene encoding human rhodopsin. We present evidence that the second class, with four members, was derived from the gene encoding the blue pigment, and that the third class, with two members, was derived from genes encoding the green pigment. The relative paucity of clones in classes 2 and 3 compared to class 1 most likely reflects the weak homology between these sequences and the bovine probe (see below).

The blue pigment gene. The four clones that constitute the second class define the 17 kb of genomic DNA shown in Fig. 1A. Nucleotide sequence analysis of the region homologous to the

bovine rhodopsin probe reveals a structure strikingly similar to that seen in the genes that encode human and bovine rhodopsins (Fig. 1B) (*5, 6*). When the DNA sequence is conceptually translated on both strands in all three reading frames, we observe five separate regions of amino acid sequence homology with bovine rhodopsin that correspond exactly to the five exons into which the human and bovine rhodopsin genes are divided (Fig. 2). These regions are bounded internally by consensus splice junction sites and are separated by intervening sequences that bear little or no homology to their rhodopsin gene counterparts. The amino acid sequence obtained by conceptually transcribing, splicing, and translating this DNA sequence can be easily aligned with the human (or bovine) rhodopsin sequence without recourse to insertion or deletion of any amino acids. The two amino acid sequences are identical at 42 percent of their residues, and homologous at an additional 33 percent (Table 1). As a consequence of this degree of homology, hydropathy plots of the two proteins are extremely similar and suggest that this new protein would form a structure with seven transmembrane segments, as has been predicted for human and bovine rhodopsins (Fig. 3) (*5–8*).

To test whether this genomic DNA segment represents a bonafide cone pigment gene we examined human retinas obtained at autopsy for messenger RNA (mRNA) products derived from it. To that end, we constructed a cDNA library synthesized from human retina mRNA and screened it for clones with sequence homology to the first of the five putative exons. The structures of two cDNA clones isolated from this library are shown in Fig. 1C. These two cDNA's confirm the intron-exon structure proposed on the basis of sequence homology with rhodopsin and demonstrate that RNA molecules derived from this gene are present in the human retina. These cDNA clones represent only one part in 30,000 in the human retina cDNA library, a frequency 150 times lower than that which we observe for cDNA clones derived from rhodopsin mRNA. This ratio corresponds roughly to the ratio of blue cones to rods, estimated at approximately 1 to 200, and is somewhat lower than the ratio of red or green cones to rods, estimated at approximately 1 to 30 (*9*). The

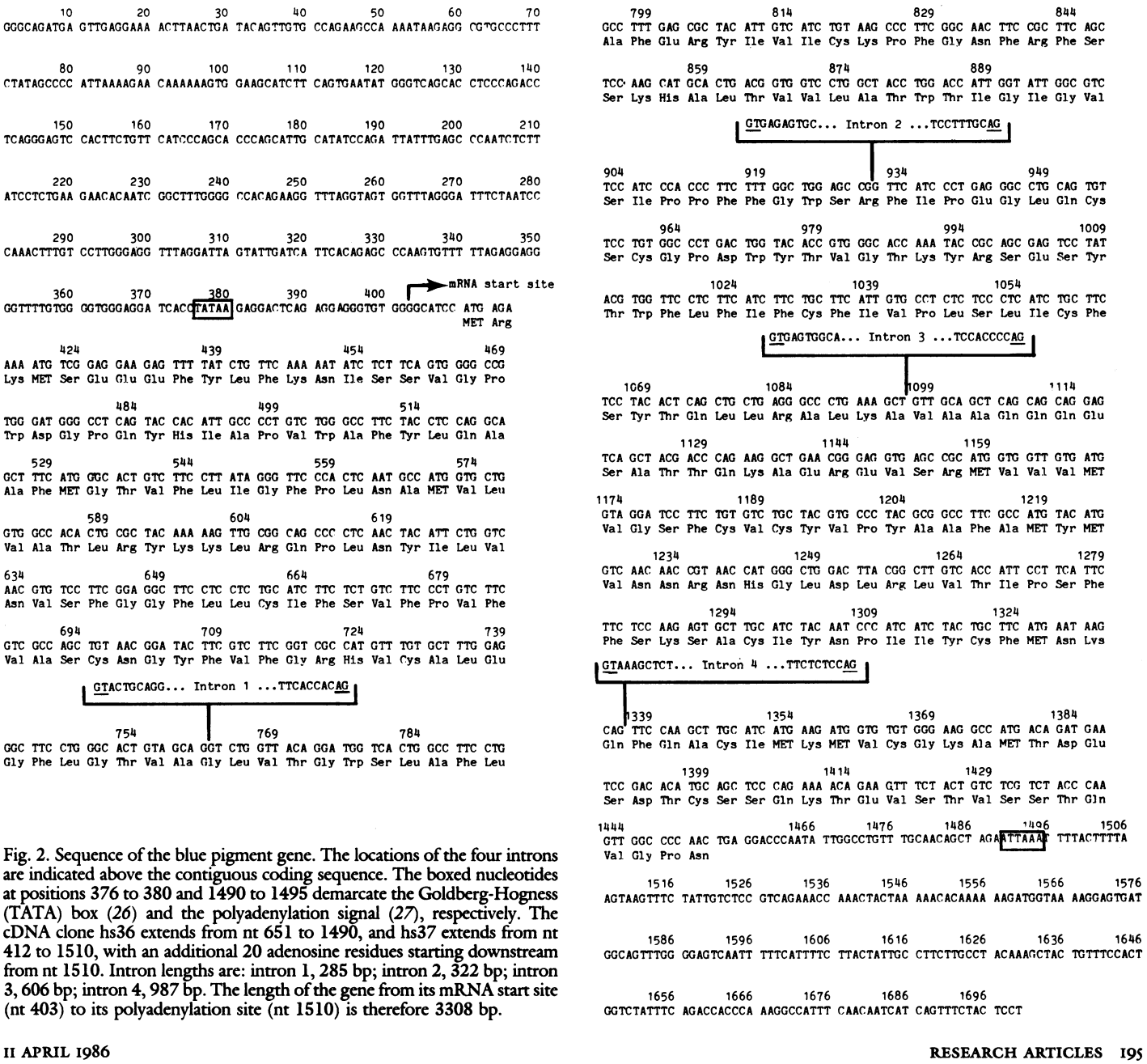

Fig. 2. Sequence of the blue pigment gene. The locations of the four introns are indicated above the contiguous coding sequence. The boxed nucleotides at positions 376 to 380 and 1490 to 1495 demarcate the Goldberg-Hogness (TATA) box (*26*) and the polyadenylation signal (*27*), respectively. The cDNA clone hs36 extends from nt 651 to 1490, and hs37 extends from nt 412 to 1510, with an additional 20 adenosine residues starting downstream from nt 1510. Intron lengths are: intron 1, 285 bp; intron 2, 322 bp; intron 3, 606 bp; intron 4, 987 bp. The length of the gene from its mRNA start site (nt 403) to its polyadenylation site (nt 1510) is therefore 3308 bp.

Fig. 3 (left). Kyte and Doolittle (*31*) hydropathy plot of the four human visual pigments. Each point on the curve represents the average hydropathy across a 21-amino-acid window centered at that position. The four curves have been aligned to optimize their sequence homology. Bars at the top demarcate the homologous regions of bovine rhodopsin predicted by Hargrave *et al.* (*7*) to reside within the hydrophobic part of the membrane. Similar predictions have been made by Ovchinnikov *et al.* (*8*) and Nathans and Hogness (*5*). Increasing hydropathy is downward.

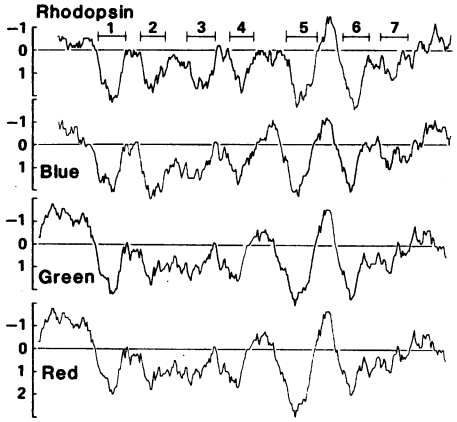

Fig. 4 (right). Analysis of the 5′ end of the blue pigment gene. The autoradiographs of each gel contain a Maxam-Gilbert sequence ladder (*23*) of an Nco I–Sal I fragment derived from gJHN11 (Fig. 1) that was labeled at the 5′ end with ^{32}P at the Nco I site (nt 567 to 572) (Fig. 2). This fragment encompasses the 5′ half of exon 1 and 2 kb of upstream sequences. (lanes 1 and 2) Products of cDNA extension by reverse transcriptase of a 5′ end-labeled (with ^{32}P) synthetic 20-nt probe after hybridization to 4 μg of human retina polysomal poly(A)$^+$ RNA (lane 1) or 4 μg of yeast transfer RNA (tRNA) (lane 2). The sequence of this 20-nt fragment corresponds to residues 552 to 571 of the noncoding strand of the blue pigment gene; that is, its 5′ end is at the point of cleavage of the above-mentioned Nco I site. (lanes 3 and 4) Products of S1 nuclease digestion after hybridization of the above 5′ end–labeled Nco I–Sal I fragment to 4 μg of human retina polysomal poly(A)$^+$ RNA (lane 3) or 4 μg of yeast transfer RNA (lane 4). The details of the methods have been described (*28*). The RNA and DNA strands are represented in the diagram by wiggly and straight lines, respectively, with the asterisk indicating the position of the ^{32}P label. The single product of cDNA extension is presumed to represent the exact 5′ end, whereas the microheterogeneity of the S1 nuclease digestion product is presumed to represent "nibbling" near the end of the RNA–DNA hybrid.

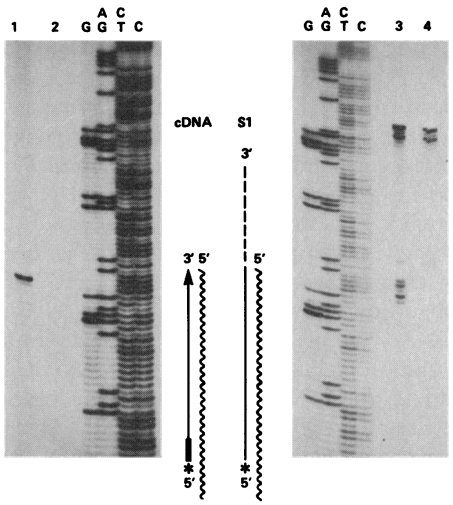

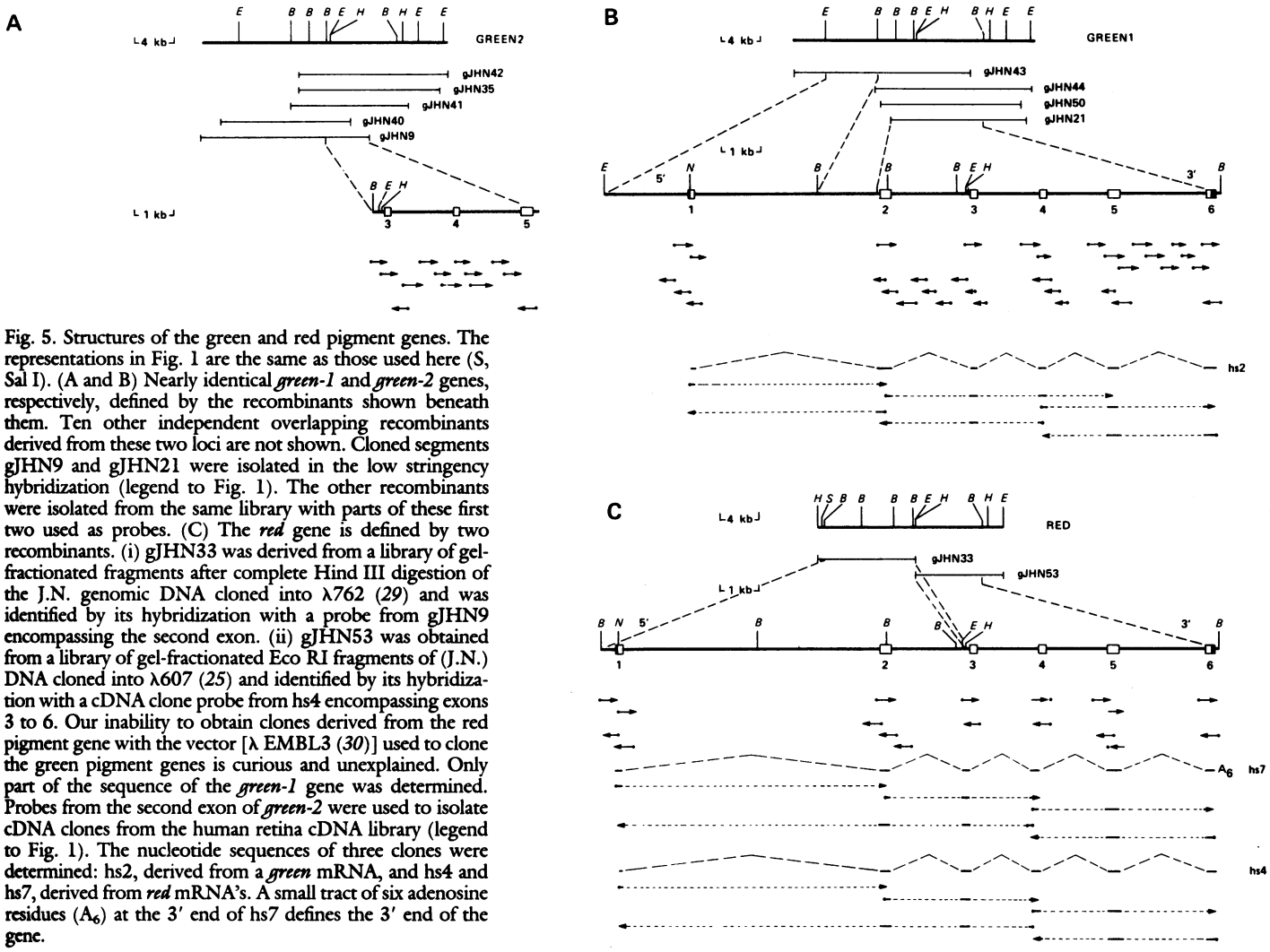

Fig. 5. Structures of the green and red pigment genes. The representations in Fig. 1 are the same as those used here (S, Sal I). (A and B) Nearly identical *green-1* and *green-2* genes, respectively, defined by the recombinants shown beneath them. Ten other independent overlapping recombinants derived from these two loci are not shown. Cloned segments gJHN9 and gJHN21 were isolated in the low stringency hybridization (legend to Fig. 1). The other recombinants were isolated from the same library with parts of these first two used as probes. (C) The *red* gene is defined by two recombinants. (i) gJHN33 was derived from a library of gel-fractionated fragments after complete Hind III digestion of the J.N. genomic DNA cloned into λ762 (*29*) and was identified by its hybridization with a probe from gJHN9 encompassing the second exon. (ii) gJHN53 was obtained from a library of gel-fractionated Eco RI fragments of (J.N.) DNA cloned into λ607 (*25*) and identified by its hybridization with a cDNA clone probe from hs4 encompassing exons 3 to 6. Our inability to obtain clones derived from the red pigment gene with the vector [λ EMBL3 (*30*)] used to clone the green pigment genes is curious and unexplained. Only part of the sequence of the *green-1* gene was determined. Probes from the second exon of *green-2* were used to isolate cDNA clones from the human retina cDNA library (legend to Fig. 1). The nucleotide sequences of three clones were determined: hs2, derived from a *green* mRNA, and hs4 and hs7, derived from *red* mRNA's. A small tract of six adenosine residues (A_6) at the 3′ end of hs7 defines the 3′ end of the gene.

presence in human retinas of mRNA derived from this gene was also confirmed by S1 nuclease and cDNA extension analyses defining the mRNA start site (Fig. 4).

Which of the three cone pigments does this gene encode? We show in the accompanying article (*4*) that it derives from human chromosome 7, whereas the rhodopsin gene derives from chromosome 3 and all of the other human cone pigment genes (described below) derive from the human X chromosome. It is well established that the loci responsible for inherited variations in the red and green mechanisms are X-linked, whereas variations in the blue mechanism are inherited in an autosomal fashion (*10*). The X-linked genes encode red and green pigments because they are specifically altered in individuals deficient in the red and green mechanisms (*4*). By elimination, then, the gene described here should encode the blue pigment. Henceforth, we refer to this gene as the blue pigment gene.

The red and green pigment genes. We turn here to the two members of the third class of clones isolated as a result of their weak homology to the bovine rhodopsin probe. These clones were mapped to the distal portion of the q arm of the human X chromosome (*4*), a region known to encompass the loci responsible for inherited defects in the red and green mechanisms. We guessed, therefore, that these two clones were derived from either the red or green pigment genes. Given the close genetic linkage (less than 5 centimorgans) between the loci for red and green defects (*10*), these genes may have arisen from a recent duplication and hence could retain a high degree of sequence homology. Using probes derived from these two clones (gJHN9 and gJHN21), we isolated 18 more genomic clones some of which are shown in Fig. 5. All of the clones are highly homologous as judged by cross-hybridization experiments, and their nucleotide sequence analysis shows more than 98 percent identity. Despite this degree of homology these recombinants can be divided into three classes on the basis of minor differences in restriction sites. We refer to these genes by their true identities—that is, red and green pigment genes—although this assignment and terminology requires data presented in (*4*).

Table 2. Exon sequence differences between genomic and cDNA clones encoding red and green pigments. No differences were seen in either the first or sixth exons. Sequences were determined only for exons 3, 4, and 5 of gJHN9 (*green-2*).

Exon	Nucleotide Position	Red Genomic gJHN33, gJHN53	Red cDNA hs4	Red cDNA hs7	Green Genomic gJHN21	Green Genomic gJHN9	Green cDNA hs2
2	688	C	C	C	T		T
2	782	A	G	G	G		G
2	794	A	A	A	G		G
2	801	A	A	A	A		T
2	825	A	G	G	G		G
2	841	C	A	A	A		A
3	947	G	G	A	A	A	G
3	951	C	C	A	A	A	C
3	959	G	G	C	C	C	G
3	1032	T	G	G	G	G	G
4	1183	T	T	T	C	C	C
4	1191	G	G	G	A	A	A
4	1192	C	C	C	G	G	G
4	1193	T	T	T	C	C	C
4	1200	A	A	A	G	G	G
5	1314	A	A	A	G	G	G
5	1317	T	T	T	C	C	C
5	1319	T	T	T	G	G	G
5	1322	G	G	G	A	A	A
5	1324	A	A	A	T	T	T
5	1329	G	G	G	T	T	T
5	1343	C	C	C	A	C	A
5	1347	A	A	A	G	G	G
5	1382	T	T	T	C	C	C
5	1386	G	G	G	C	C	C
5	1420	A	A	A	T	T	T

The first two classes of clones shown in Figs. 5, A and B, and labeled *green-1* and *green-2* have identical Bam HI, Eco RI, Hind III, and Sal I restriction maps. The third class, labeled *red* (Fig. 5C), has only two members (gJHN33 and gJHN53) and differs from the first two classes with respect to Bam HI, Eco RI, Hind III, and Sal I restriction sites in only the leftmost 10 kb. Genomic DNA blots hybridized with probes throughout these cloned segments reveal no bands other than those predicted by the three restriction maps shown in Fig. 5. An example of restriction site differences that distinguish all three classes is shown in Fig. 6. In this experiment the 1.8-kb Bam HI fragment just to the right of exon 2 (which all three classes possess) was isolated from those clones that include this region. The fragments were then digested with Bst NI, ^{32}P end-labeled, and subjected to electrophoresis on an acrylamide gel. The Bst NI digestion patterns, four examples of which are shown in Fig. 5, fall into three classes. The same division into three classes is also observed after Hpa II digestion of these 1.8-kb Bam HI fragments. gJHN53 (*red*, Fig. 5C) was distinguished from the *green-1* and *green-2* classes on the basis of an Rsa I restriction site difference in exon 5. In comparing those exons (numbers 3, 4, and 5) for which sequences have been determined from all three classes of clones, *green-1* and *green-2* show only a single silent nucleotide substitution, whereas *red* differs from *green-1* and *green-2*, respectively, by 20 and 19 nucleotide substitutions out of 578 nucleotides, which cause 12 amino acid substitutions (Table 2). These data suggest that the two classes labeled *green-1* and *green-2* represent two copies of a single type of gene (green pigment gene), whereas the class labeled *red* represents a different but closely homologous type (red pigment gene).

Sequence analysis of these three classes of clones (Fig. 6) reveals blocks of homology to rhodopsin that correspond exactly to the five exons of the rhodopsin gene; these are labeled exons 2 to 6 in Fig. 5.

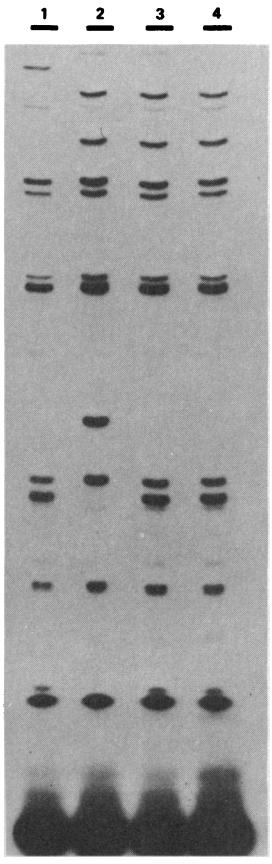

Fig. 6. Restriction site differences define three classes of X-linked recombinants. The 1.8-kb Bam HI fragment located just to the right of exon 2 (Fig. 5) was purified from gJHN21 (lane 1, *green-1*), gJHN33 (lane 2, *red*), gJHN35 (lane 3, *green-2*), and gJHN41 (lane 4, *green-2*), recut with Bst N1, ^{32}P–end-labeled, subjected to electrophoresis (5 percent acrylamide gel), and autoradiographed.

However, at the 5′ end of exon 2 there is an abrupt break in the homology with rhodopsin at a position corresponding to the 20th amino acid from rhodopsin's amino terminus. Analysis of *green* and *red* cDNA clones isolated from the human retina cDNA library demonstrates that an additional exon, labeled 1, is spliced onto the second exon just upstream of this point of sequence divergence (Figs. 5 and 7). This first exon, which encodes amino acids 1 to 37 (starting from the only in frame methionine codon), has no homolog in the rhodopsin gene or the blue pigment gene but is present in both the red and green pigment genes.

Sequence analysis of these cDNA clones confirms the intron-exon structure predicted on the basis of sequence homology with rhodopsin. This analysis demonstrates that both red and green sequences are transcribed into RNA in the human retina. In the human retina cDNA library the abundance of cDNA clones homologous to red and green pigment genes is 1 part in 3000, 1/15th the abundance of cDNA clones derived from rhodopsin mRNA. This ratio of cDNA clones is comparable to the ratio of red and green cones to rods (*9*). The presence in human retinas of mRNA derived from these genes was also confirmed by S1 nuclease and cDNA extension experiments defining the mRNA start site (Fig. 7).

The cDNA and genomic DNA sequences show regions of greater and lesser variability (Table 2). In the first and sixth exons all of the sequences that have been examined are identical. The fourth and fifth exon sequences divide the cDNA clones into two classes that correspond to the two genomic DNA classes. However, second and third exon sequences show scattered differences such that no two cDNA sequences are identical and no cDNA agrees exactly with any

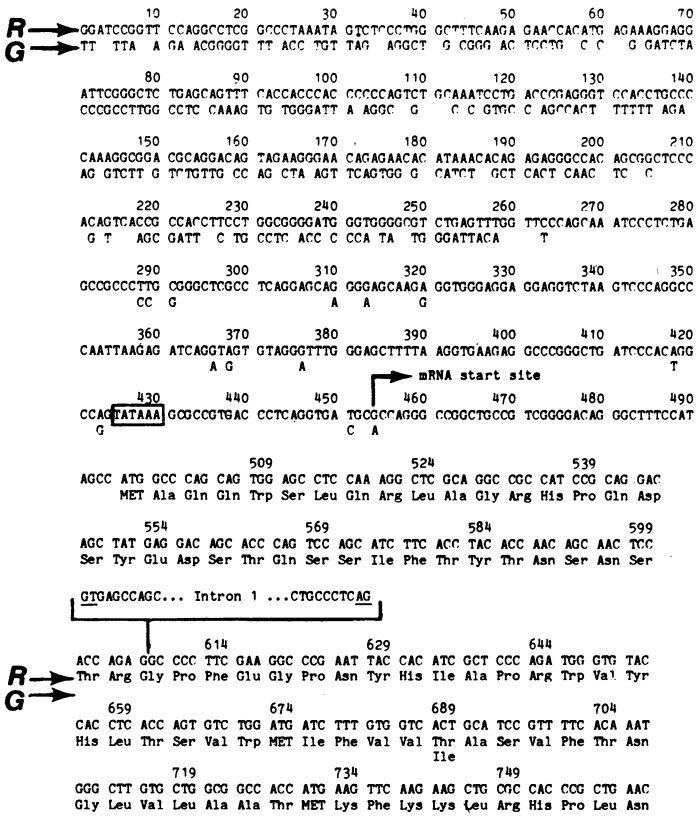

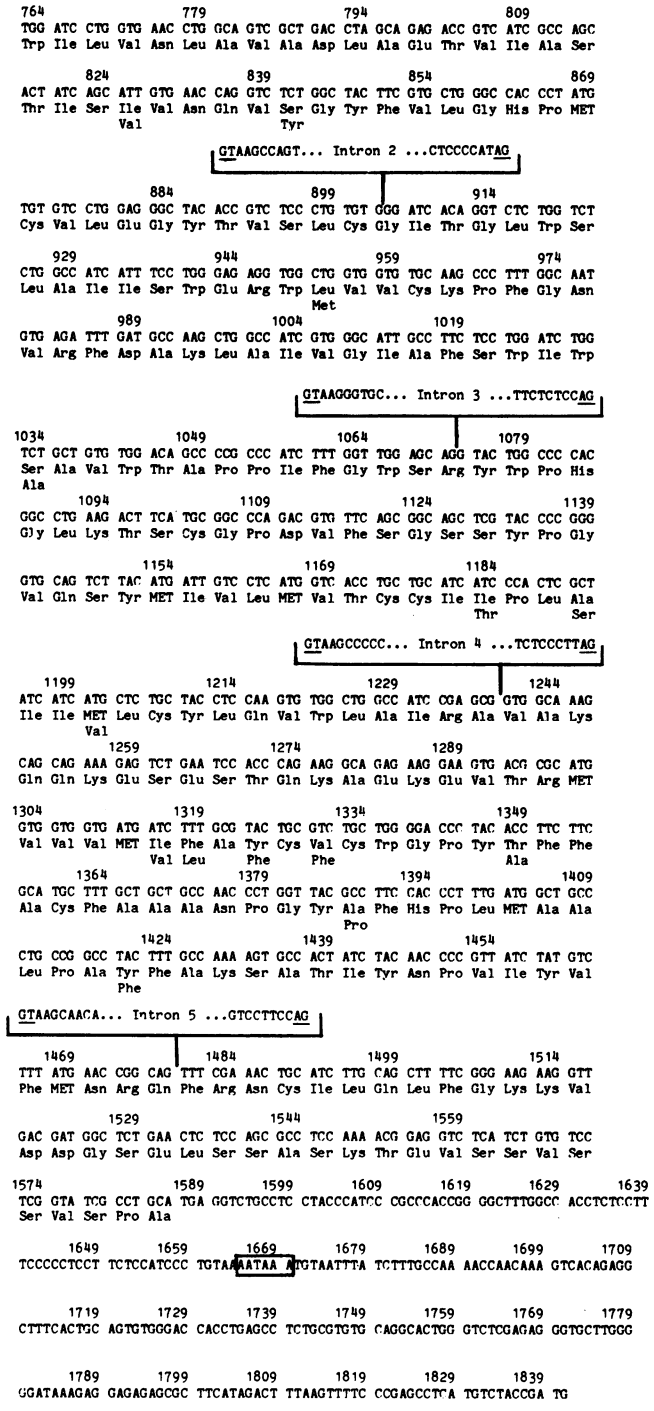

Fig. 7. Sequences of the green and red pigment genes. The locations of the five introns are indicated above the contiguous coding region; these locations and adjacent intron sequences are identical in both genes. The upper sequence is that of the red pigment gene, the lower sequence is that of the green pigment gene. Identical nucleotide or amino acid residues are left blank in the lower sequence. In the coding region, the single DNA sequence shown is that of the red pigment gene; those nucleotide differences that correspond to the green pigment gene coding region sequence are shown in Table 2. The boxed nucleotides at positions 425 to 430 and 1665 to 1670 demarcate the Goldberg-Hogness or TATA (*26*) box and the polyadenylation signal (*27*), respectively. The mRNA's transcribed from both red and green pigment genes start at nt 454 as determined by S1 nuclease and cDNA extension experiments (methods described in legend to Fig. 4). Complementary DNA clone hs2 extends from nt 537 to 1661, hs4 extends from nt 561 to 1682, and hs7 extends from nt 455 to 1694 with an additional six adenosine residues starting at position 1694, which therefore marks the 3′ end of the red mRNA. Intron lengths are: intron 1, 4.65 ± 0.1 kb (green) and 6.60 ± 0.1 kb (red); intron 2, 1988 bp (green) and 2.0 ± 0.1 kb (red); intron 3, 1476 bp (green) and 1.5 ± 0.1 kb (red); intron 4, 1651 bp (green) and 1.6 ± 0.1 kb (red); intron 5, 2271 bp (green) and 2.3 ± 0.1 kb (red). The lengths of the green and red pigment genes, from the mRNA start site to the polyadenylation site, are 13.3 kb and 15.2 kb, respectively. This length difference results from a difference in lengths of intron 1.

genomic DNA sequence. Because the cDNA clones were produced from an mRNA population prepared from several dozen retinas, we ascribe these differences to polymorphism.

We have grouped together gJHN33 and gJHN53 as two parts of a single gene even though they overlap for only 43 bp (Fig. 5C). This assignment rests not only on the finding of differences that distinguish them from *green-1* and *green-2* clones, but also on the observation that different color normal individuals always have a constant stoichiometry of fragments corresponding to gJHN33 and gJHN53. As discussed below, green pigment genes vary in number from one individual to the next and in each case the variation is limited to those fragments corresponding to the *green-1* and *green-2* restriction maps. Furthermore, as we have shown in (*4*), six different G^-R^+ dichromats (G^-, absent green sensitivity; R^+, normal red sensitivity) are missing all of the material corresponding to the *green-1* and *green-2* restriction maps but retain that corresponding to the *red* restriction map with the normal fragment stoichiometry.

Like the blue pigment, the red and green pigments can be aligned with rhodopsin without any insertions or deletions. They also share about the same degree of homology with rhodopsin as does the blue pigment (Table 1) and their hydropathy plots define the same set of maxima and minima (Fig. 3).

Variations in gene number. All of the genomic clones studied derive from the DNA of a phenotypically normal male (J.N.). Therefore, the three classes of clones defining the *green-1*, *green-2*, and *red* genes must derive from a single X chromosome. A priori we would have expected only two X-linked visual pigment genes—one encoding the red pigment and one the green pigment. The surprising finding of three genes led us to ask whether other X chromosomes had the same or different numbers of genes. A set of three genomic DNA blots in which various restriction enzymes and hybridization probes were used are shown in Fig. 8; those tracks labeled with a given number contain DNA derived from the same color-normal male. We have examined DNA from 18 normal males, 14 of which are shown here. Only fragments that bear a high degree of homology to the probes are visualized: these include all of the X-linked gene sequences but do not include rhodopsin or the blue pigment gene. In each case all of the predicted hybridizing fragments are present; however, their intensity varies from sample to sample. To control for slight variations in the amount of DNA loaded per track, we first compared the ratios of the intensities of the various bands within each track. In Fig. 9, we show a histogram of these values for the Eco RI digest shown in Fig. 8B; these ratios are quantized at integral values. To facilitate comparisons between different tracks, we measured the amount of DNA per track by reprobing this filter with labeled total human genomic DNA. The intensity of the resultant smear is proportional to the amount of DNA present. This analysis reveals that each sample has approximately the same amount (1.00 ± 0.20, mean ± SD) of hybridization in those fragments labeled A_r. (See legend to Fig. 8 for explanation of the lower intensity of bands in lane 14.) In contrast, those fragments labeled A_g are present at either one, two, or three times the intensity of A_r. We also observe corresponding variations in the ratios $B_g:B_r$, $C_g:C_r$, and $D_g:D_r$, although these B, C, and D ratios do not cluster as tightly as $A_g:A_r$ ratios. If we assume that the variation in the number of green pigment genes occurs in steps of one, then this variation serves to calibrate the absolute number of genes present and implies the existence of only a single red pigment gene per X chromosome.

How might this variation in gene number arise? A simple model in which a head-to-tail arrangement—presumably the product of an ancient gene duplication—predisposes the genes to undergo un-

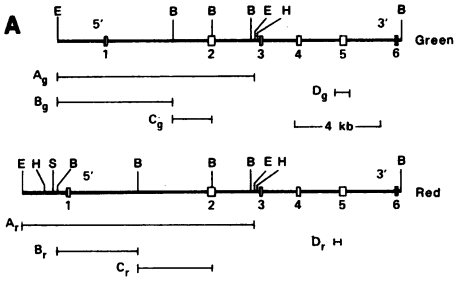

Fig. 8. (A) Restriction maps of green and red pigment genes showing fragments visualized by Southern blotting of genomic DNA. The probes used to visualize these fragments are more than 98 percent identical to both red and green pigment genes. A_g and A_r are two Eco RI fragments derived from the green and red pigment genes, respectively, and are visualized with a probe from exon 2. Fragments B_g and B_r, and fragments C_g and C_r result from Bam HI and Eco RI double digestion and are visualized with a probe encompassing exon 1 and the 5′ half of exon 2. D_g and D_r are fragments resulting from Rsa I digestion; they share a common left border but differ on their right borders because the green pigment gene lacks but the red pigment gene possesses an Rsa I site in the fifth exon. They are visualized with a probe from the 3′ end of the fourth intron. (B–D) Three genomic Southern blots of DNA from 14 color-normal males. Each number refers to a single individual whose DNA is present in that lane. (B) Eco RI; (C) Bam HI and Eco RI; (D) Rsa I. Lanes 3 and 4 are reversed in B with respect to C and D. Approximately 10 μg of DNA, digested with the indicated enzymes, was placed on each lane. By mistake, lane 14 in (B), which contains DNA from J.N., received only 5 μg; repeats of this sample are shown in (*4*, figure 3). Filters were hybridized and washed under standard conditions (*25*) and exposed to preflashed film at −70°C with an intensifying screen.

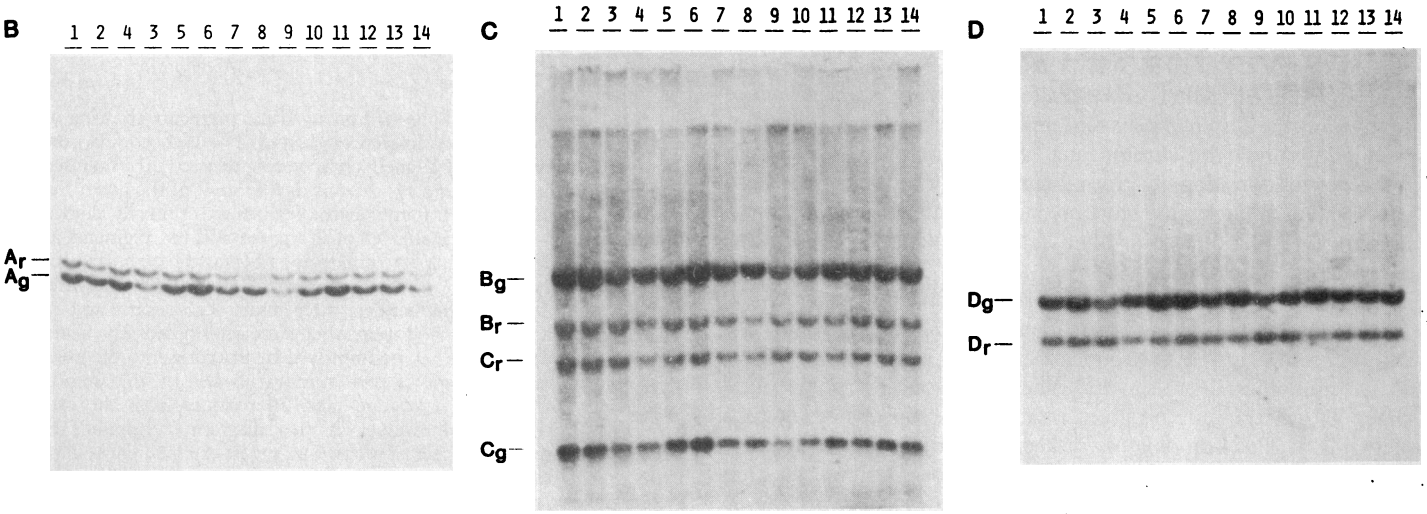

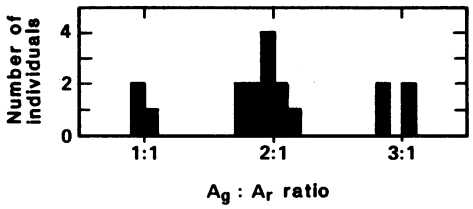

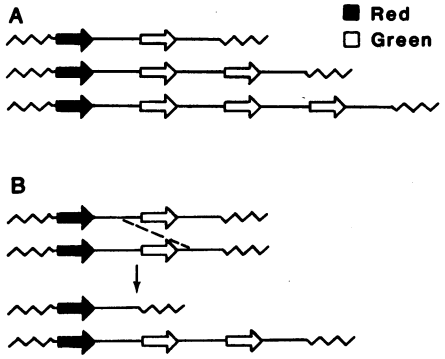

Fig. 9 (left). Histogram of A_g:A_r ratios in DNA from 18 normal males. The autoradiogram shown in Fig. 8B and an analogous one with DNA from four other color-normal males were scanned, the areas under the peaks were measured, and the A_g:A_r peak area ratios were calculated. Fig. 10 (right). (A) Proposed arrangement of green and red pigment genes in color-normal males. Each arrow represents a single gene; the base corresponds to the 5′ end and the tip to the 3′ end. The thin straight lines that lie to the 3′ side of each gene represent duplicated intergenic spacers, which are presumed to be highly homologous, whereas the zigzag lines indicate flanking single-copy DNA. The distance between genes has not been determined. (B) A possible mechanism for changing the copy number of green pigment genes. Unequal crossing-over in the intergenic region produces one chromosome with fewer and one chromosome with more green pigment genes.

equal recombination is shown in Fig. 10. The intergenic exchange shown would give rise to one product with one red and two green pigment genes and a second product with only a red pigment gene. This second product would be expected to confer on a hemizygous male a phenotype of G^-R^+ dichromacy. We have shown that this is indeed the case (*4*).

The presence of only one red pigment gene per chromosome in color-normal males can be explained by supposing that this gene lies at the very edge of the repeated array (Fig. 10). In this position, its complete duplication or deletion by homologous but unequal recombination is impossible. Its placement at the 5′ rather than the 3′ end of the array is dictated by two considerations. In certain color-blind subjects the 3′ proximal part of the red pigment gene may be duplicated via a homologous exchange, whereas the 5′ region is never duplicated or deleted (*4*). This is the expected result of unequal recombination if the 5′ end of the red pigment gene is at the edge of the array, whereas the reciprocal result would be expected were the 3′ end to reside at the edge of the array. In contrast to these alterations of the red pigment gene, all parts of the green pigment gene—including entire genes—may be either duplicated or deleted (*4*).

The second consideration is that the nucleotide sequence upstream from the 5′ end of the red pigment gene becomes completely divergent from that for the green pigment gene after the first 195 upstream nucleotides (nt) (Fig. 7; the first 195 nt are 93 percent conserved between the two genes). Consequently, placement of the red pigment gene either at the 3′ end of the array, or within it, would interrupt its tandem repetition. This divergence of upstream sequences is not surprising in that the differential expression of these genes in different cone cells may be regulated at the level of transcription initiation. The sequence differences in their upstream regions—both within the first 195 nt and further upstream—may be indicative of sequence elements regulating that initiation.

We have not yet isolated DNA spanning the interval between any pair of X-linked genes, and therefore have no direct evidence concerning the distance between genes or their relative order and orientation along the chromosome. However, the observed high frequency of variation in green pigment gene number, the high conservation of nucleotide sequence, and the nature of the red-green hybrid genes found in color-blind subjects (*4*) suggest the tandem arrangement shown in Fig. 10.

Evolution of the visual pigments. In Table 1, we show the percentage of amino acids that are identical and homologous in each pairwise comparison of the four human visual pigments, and in Fig. 11 we show these identities and differences along the polypeptide chain. Clearly the red and green pigments are highly homologous (Fig. 11D). This homology is in keeping with the demonstration (*11*) that Old World monkeys and humans appear to have the same green and red cone pigments, presumably encoded on the X chromosome, whereas New World monkeys have only a single long wavelength visual pigment encoded on the X chromosome. This comparison implies that the generation of red and green pigment genes, after a duplication event, occurred after the split between New and Old World primates, some 30 to 40 million years ago (*12*). If, for purposes of comparison, we lump together the human red and green pigments as representatives of a long wavelength pigment, then the comparisons in Table 1 suggest that short wavelength (blue), long wavelength (red and green), and rod pigments all diverged from a common ancestor at about the same time. If the amino acid sequence divergence between human and bovine rho-

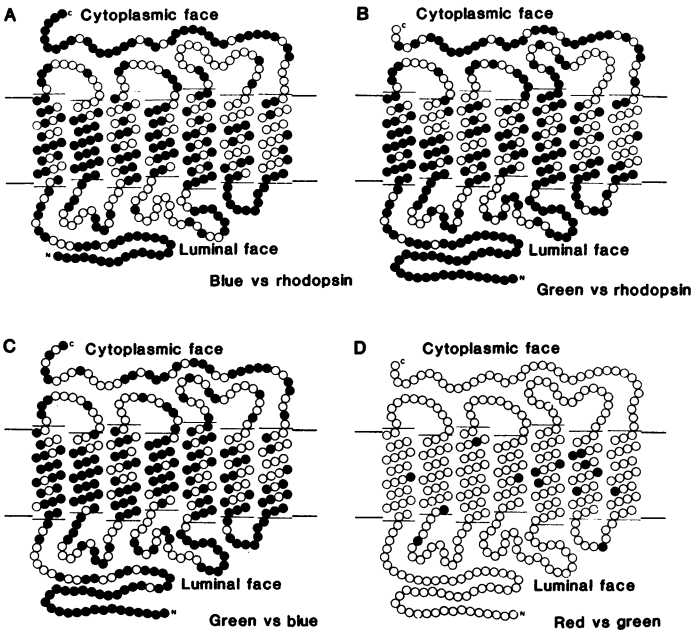

Fig. 11. Pairwise comparisons of human visual pigments showing amino acid identities (white) and differences (black). For each comparison, the amino acids were optimally aligned, an operation that required no insertions or deletions except in comparing the carboxyl termini of the green (or red) and blue pigments. When intramembrane regions are optimally aligned, the amino-proximal tails (luminal face) of the green and red pigments are 16 amino acids longer than that for rhodopsin, whereas the carboxyl-proximal tails (cytoplasmic face) are of the same length. The amino- and carboxyl-proximal tails of the blue pigment are three amino acids shorter and longer, respectively, than that for rhodopsin when similarly aligned. The alignment of green (or red) and blue can be improved by inserting into the green (or red) pigment sequence gaps of two amino acids and of one amino acid, respectively, at positions 4 residues and 29 residues from the carboxyl terminus. The number of residues in each diagram corresponds to the greatest extent to which either of the two pigments extends. These diagrams are modified versions of the schematic diagram for bovine rhodopsin devised by Hargrave *et al.* (*7*).

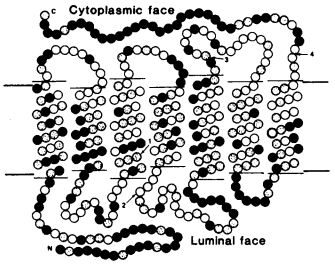

Fig. 12. Locations of identical (white), conserved (stippled), and nonconserved (black) amino acids in comparisons of all four human visual pigments and bovine rhodopsin. Each position is scored by the least homologous substitution observed there; for example, if four of the five sequences have conservative substitutions and the fifth has a nonconservative one, then that position is scored as nonconserved. The criteria for conservative substitutions are given in the legend of Table 1. The residue with the enhanced outline is Lys^{296} in rhodopsin and is the site at which 11-*cis*-retinal is covalently linked (*14*). Intron locations for the genes encoding human and bovine rhodopsins and the blue pigment are shown by numbered arrows.

dopsins [1 percent per 10 million years (*5, 6*)] is used to calibrate sequence differences among cone pigments, then the point of divergence of these three pigments is estimated to be more than 500 million years. The finding that *Drosophila melanogaster* rhodopsin (*13*) diverges even more than the cone pigments puts an upper limit of approximately 1×10^9 years on the split between rod and cone pigments.

Functional implications of the cone pigment sequences. All pairwise comparisons between shortwave, longwave, and rod pigments show between 40 and 45 percent amino acid identity. If the amino acid identities between any two pigments were uncorrelated with those of the third, we would expect 17.6 ± 2.6 percent (mean ± SD) of the amino acids to be shared by all three sequences. We observe instead that 27 percent (94/348) are shared by all three. This high degree of sequence correlation is typical of comparisons between members of a protein family and serves to highlight the residues that may be critical to structure and function (*12*) (Fig. 12). All of the human pigments have a lysine corresponding to position 296 of rhodopsin, the site of covalent attachment to 11-*cis*-retinal (*14*). The three cytoplasmic loops, likely points of contact with transducin, are also conserved. The carboxyl terminal regions, although not well conserved, all contain serine and threonine residues which, in bovine rhodopsin, are the sites of light-dependent phosphorylation by rhodopsin kinase (*15*). Phosphorylation of these residues turns off rhodopsin activity (*15, 16*); by analogy we suppose that cones may also have a kinase that turns off light-activated cone pigments (*17*). Interestingly, in this carboxyl terminal region the three cone pigments are significantly more similar to one another than they are to rhodopsin (Fig. 11). The amino terminal regions, which are highly divergent, each contain at least one canonical *N*-glycosylation site, Asn-X-Ser or Thr (X is any amino acid residue). Finally, two regions, the second luminal loop and the seventh transmembrane segment, which are conserved between the evolutionarily distant mammalian and *Drosophila* rhodopsins (*13*), are also conserved among the human visual pigments. Perhaps these regions play an important role in visual pigment structure or function.

Tuning the absorption spectrum of 11-*cis*-retinal. How might the various opsins modify the environment of 11-*cis*-retinal so that its absorption spectrum is appropriately shifted? A large body of experimental and theoretical data supports the following model (*18*): (i) retinal is attached to the ε-amino group of lysine by way of a protonated Schiff's base; (ii) in photoexcited retinal there is a transfer of positive charge from the Schiff's base nitrogen to retinal's conjugated pi-electron system; and (iii) positively or negatively charged amino acids near the pi-electron system preferentially destabilize or stabilize, respectively, the excited state, whereas positively or negatively charged amino acids near the Schiff's base nitrogen preferentially destabilize or stabilize, respectively, the ground state.

How well does this model fit the sequence data? Without a three-dimensional structure of a visual pigment we can only make educated guesses as to which residues contact retinal. Since retinal is bound to the middle of the seventh transmembrane segment and lies approximately in the plane of the membrane, it is possible that it may at various points contact most if not all of the transmembrane segments. Present evidence suggests that the seven transmembrane segments of rhodopsin form a palisade of helical rods around retinal in a manner analogous to that formed by bacteriorhodopsin (*19*). The charged residues predicted to lie in transmembrane segments are highlighted in Fig. 13. Both the number and positions of these residues differ between the long wavelength, short wavelength, and rod pigments. In each case the differences are confined to helices 2 to 5. (Helices are numbered from amino to carboxyl terminus.) The net intramembrane charge of the blue pigment (λ_{max} = 420 nm) is +1, that of rhodopsin (λ_{max} = 495 nm) is 0, and that of the green and red pigments (λ_{max} = 530 and 560 nm, respectively) is −1. These charge differences may be responsible, at least in part, for spectral absorption differences.

The red and green pigments have identical intramembrane charge distributions. Indeed, all of the amino acid substitutions that distinguish them, most of which are in the transmembrane region (Fig. 11D), involve uncharged residues. The most extreme type of substitution is the replacement of an amino acid with a hydroxyl for one without (such as tyrosine for phenylalanine). We can rationalize the subtlety of these differences by recalling that the difference in energy between photons of 530 and 560 nm is only 3 kilocalories per mole. Perhaps the intrinsic dipole moment of some amino acid side chains (such as that of tyrosine) provides the requisite electrostatic perturbation (*20*). Alternatively, polarization of a hydroxyl in one pigment may transmit to retinal part of the effects of a more distant charge, whereas in another pigment retinal is shielded from these effects.

In sum, our experiments verify the hypothesis that the three human cone pigments and the rod pigment rhodopsin form a single family of homologous proteins encoded by the corresponding

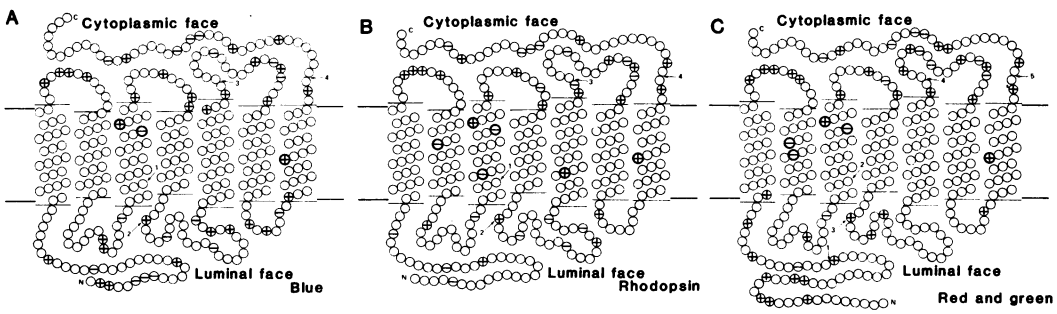

Fig. 13. Charged amino acids in transmembrane regions of the human visual pigments. All of the charged amino acids are indicated; those that are most likely to interact with retinal are emphasized with darker lines. Intron positions are indicated by numbered arrows.

members of a family of genes. The data reveal a high degree of homology between green and red pigment genes, each of which shares a lower degree of homology with the blue pigment gene comparable to the lower homology that each of the cone pigment genes shares with the rhodopsin gene. These results indicate that the evolution of the human visual pigment genes proceeded by the early divergence from a common ancester of three genes, two of which generated the rhodopsin and blue pigment genes, while the third was duplicated in a much more recent evolutionary event to yield the green and red pigment genes. The number of green pigment genes per X chromosome is highly variable among different color normal individuals, whereas the red pigment gene number is constant and probably one. Such a variable-constant relation between the green and red pigment gene numbers is consistent with a model in which these genes are arranged in a head-to-tail tandem array with the single red pigment gene occupying the 5′ terminal position. Further evidence favoring this model is presented in (*4*).

The deduced amino acid sequences of the cone pigments and of rhodopsin are consistent with a model of retinal tuning by interactions with neighboring charged amino acids. A variety of experiments, including tests of this tuning model, will be possible if functional visual pigments can be expressed from these cloned DNA's and derivatives of them. Isolation of rod (*5, 6*) and cone pigment genes is also a first step in addressing the fascinating question of how during development a photoreceptor cell chooses to produce one of the four visual pigments.

REFERENCES AND NOTES

1. B. K. Fung and L. Stryer, *Proc. Natl. Acad. Sci. U.S.A.* **77**, 2500 (1980); B. K. Fung, J. B. Hurley, L. Stryer, *ibid.* **78**, 152 (1981); R. Yee and P. A. Liebman, *J. Biol. Chem.* **253**, 8902 (1978); E. E. Fesenko, S. S. Kolesnikov, A. L. Lyubarsky, *Nature (London)* **313**, 310 (1985).
2. H. J. A. Dartnall, *Brit. Med. Bull* **9**, 24 (1953).
3. R. Boynton, *Human Color Vision* (Holt, Rinehart, & Winston, New York, 1979); J. D. Mollon and L. T. Sharpe, Eds., *Colour Vision* (Academic Press, New York, 1983).
4. J. Nathans, T. P. Piantanida, R. L. Eddy, T. B. Shows, D. S. Hogness, *Science* **232**, 203 (1986).
5. J. Nathans and D. S. Hogness, *Cell* **34**, 807 (1983).
6. ———, *Proc. Natl. Acad. Sci. U.S.A.* **81**, 4851 (1984).
7. P. A. Hargrave *et al.*, *Biophys. Struct. Mech.* **9**, 235 (1983).
8. Yu. A. Ovchinnikov *et al.*, *Bioorg. Khim.* **8**, 1424 (1982).
9. R. E. Marc and H. G. Sperling, *Science* **196**, 454 (1977); H. J. A. Dartnall, J. K. Bowmaker, J. D. Mollon, in *Colour Vision*, J. D. Mollon and L. T. Sharpe, Eds. (Academic Press, New York, 1983), p. 69; G. Osterberg, *Acta Ophthalmol.* **6** (suppl.), 1 (1935); E. P. McCrane, F. M. de Monasterio, S. J. Schein, R. C. Caruso, *Invest. Ophthalmol. Visual Sci.* **24**, 1449 (1983).
10. J. Francois, *Heredity in Ophthalmology* (Mosby, St. Louis, MO, 1961); H. Kalmus, *Diagnosis and Genetics of Defective Colour Vision* (Pergamon, New York, 1965).
11. G. H. Jacobs, *Vision Res.* **23**, 239 (1983); J. K. Bowmaker, J. D. Mollon, G. H. Jacobs, in *Colour Vision*, J. D. Mollon and L. T. Sharpe, Eds. (Academic Press, New York, 1983), p. 57.
12. M. O. Dayhoff, *Atlas of Protein Sequence and Structure* (National Biomedical Research Foundation, Washington, DC, 1972), vol. 5.
13. J. E. O'Tousa *et al.*, *Cell* **40**, 839 (1985); C. S. Zuker, A. F. Cowan, G. M. Rubin, *ibid.*, p. 851.
14. D. Bownds, *Nature (London)* **216**, 1178 (1967); E. Mullen and M. Akhtar, *FEBS Lett.* **132**, 261 (1981); J. K. Wang, J. H. McDowell, P. A. Hargrave, *Biochemistry* **19**, 5111 (1980).
15. H. Kuhn and W. J. Dreyer, *FEBS Lett.* **20**, 1 (1972); D. Bownds, J. Dawes, J. Miller, M. Stahlman, *Nature (London) New Biol.* **237**, 125 (1972); P. A. Hargrave, *Progress in Retinal Research* (Pergamon Press, New York, 1982), vol. 1.
16. H. Kuhn, S. W. Hall, U. Wilden, *FEBS Lett.* **176**, 473 (1984); P. A. Liebman and E. N. Pugh, *Nature (London)* **287**, 734 (1980).
17. A. E. Walter, T. A. Shuster, D. B. Farber, *Invest. Ophthalmol. Visual Sci.* **26** (suppl.), 291 (1985).
18. A. Kropf and R. Hubbard, *Ann. N.Y. Acad. Sci.* **74**, 266 (1958); R. Mathies and L. Stryer, *Proc. Natl. Acad. Sci. U.S.A.* **73**, 2169 (1976); B. Honig, A. D. Greenberg, U. Dinur, T. G. Ebrey, *Biochemistry* **15**, 4593 (1976); B. Honig *et al.*, *J. Am. Chem. Soc.* **101**, 7084 (1979); M. Sheves, K. Nakanishi, B. Honig, *ibid.*, p. 7086.
19. R. Henderson and P. N. T. Unwin, *Nature (London)* **257**, 28 (1975); Yu. A. Ovchinnikov, *FEBS Lett.* **148**, 179 (1982).
20. T. R. Hays, S. H. Lin, H. Eyring, *Proc. Natl. Acad. Sci. U.S.A.* **77**, 6314 (1980).
21. W. D. Benton and R. W. Davis, *Science* **196**, 180 (1977).
22. P. W. J. Rigby, M. Dieckmann, C. Rhodes, P. Berg, *J. Mol. Biol.* **113**, 237 (1977).
23. A. Maxam and W. Gilbert, *Proc. Natl. Acad. Sci. U.S.A.* **74**, 560 (1977).
24. T. V. Huynh, R. Young, R. W. Davis, in *DNA Cloning, A Practical Approach*, D. M. Glover, Ed. (IRL Press, London, 1985), vol. 1, p. 49.
25. R. W. Davis, D. Botstein, J. R. Roth, Eds., *Advanced Bacterial Genetics* (Cold Spring Harbor Laboratory, Cold Spring Harbor, NY, 1980).
26. M. L. Goldberg, thesis, Stanford University (1979); R. Breathnach and P. Chambon, *Annu. Rev. Biochem.* **50**, 349 (1981).
27. J. R. Nivens, *Annu. Rev. Biochem.* **52**, 441 (1983).
28. M. A. T. Muskavitch and D. S. Hogness, *Cell* **29**, 1041 (1982).
29. N. E. Murray, W. J. Brammer, K. Murray, *Mol. Gen. Genet.* **150**, 53 (1977).
30. A.-M. Frischauf, H. Lehrach, A. Poustka, N. Murray, *J. Mol. Biol.* **170**, 827 (1983).
31. J. Kyte and R. F. Doolittle, *ibid.*, *Biol.* **157**, 105 (1982).
32. A. L. Lehninger, *Biochemistry* (Worth, New York, 1975).

33. We thank our colleagues who served as subjects in these experiments; Willie Brown, Kris Johnson, and Dr. Jeffrey Sklar for assistance in obtaining autopsy specimens of human eyes; and Dr. Lubert Stryer for his insight and enthusiasm throughout the course of this work. J.N. is a trainee of the Medical Scientist Training Program of the National Institutes of Health. Supported by a grant from the National Eye Institute (D.S.H.).

14 January 1986; accepted 21 February 1986